Electrical Stimulation of Brain using a realistic 3D Human Head Model: Improvement of Spatial Focality

Abhishek Datta, Maged Elwassif and Marom Bikson[*]
The City College of the CUNY, New York, NY
*T-403 B Steinman Hall, Grove School of Engineering, The City College of the CUNY, 160 Convent Avenue, New York, NY 10031, bikson@ccny.cuny.edu

Abstract: We calculated the spatial distribution of the electric fields induced in the brain during transcranial current stimulation (TCS). The spatial focality obtained using 'concentic-ring' configurations is investigated using a realistic MRI derived 3D finite element model of the human head.

Two disc electrode configurations were simulated: (1) distant-bipolar and (2) reduced concentric-ring. For each configuration, we compared the spatial focality of stimulation.

The distant-bipolar configuration, which is comparable to commonly used TCS protocols, resulted in diffuse (un-focal) modulation. The reduced concentric-ring results in higher spatial focality at the expense of increased total surface current.

Superficial cortical neurons may be thus selectively targeted using a concentric-ring configuration.

Keywords: tDCS, TES, ECT, Finite Element Modelling, Human Head Model, MRI

1. Introduction

Transcranial current stimulation (including TES, CES, ECT, tDCS) involves the application of currents delivered through the scalp to modulate brain activity [1]–[3]. Clinical transcranial current stimulation (TCS) is being actively explored as a non-invasive therapeutic option for the treatment of neurological and psychiatric disorders including depression, stroke, epilepsy, learning disorders and for relieving pain.

A critical factor for TCS efficacy and safety is the spatial focality of induced neuronal modulation. TCS is considered to be poorly focused using common 'distant-bipolar' electrode configuration [4]-[6]. Spatial focality has been proposed to increase significantly using concentric-ring configuration [6]. In order to practically implement the concentric-ring

configuration, we approximated the ring using four disks arranged in a circular fashion around one center electrode (i.e. the 4 X 1 concentric-ring electrode configuration). In this paper, we compared the focality of distant-bipolar stimulation with the novel 4 X 1 electrode configuration.

The TCS induced electric fields are calculated using an anatomically accurate MRI derived model of the human head. The objective of this study was to analyze the induced electric fields for the electrode configurations, which will enable the 'rational' [7] development of TCS research and clinical protocols.

2. Methods

2.1 3D MRI derived FEM model

The volume conductor model used in this study was created from high resolution 3T MRI scans at 1 mm X 1 mm X 1 mm spacing. The head was segmented into four compartments representing the brain tissue (Figure 1a,) the cerebrospinal fluid (Figure 1b), the skull and the skin respectively. In-built segmentation tools and smoothing algorithms of SIMPLEWARE Ltd. were used.
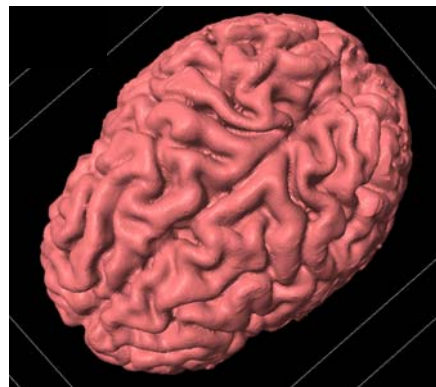

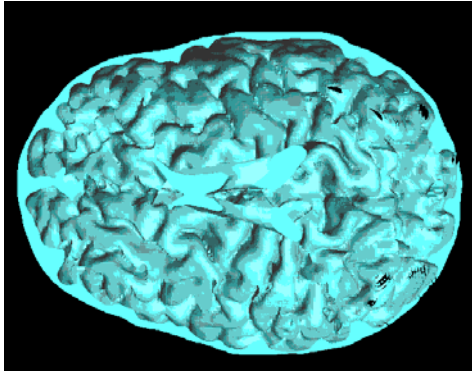**Figure 1a**. Finite element (FE) brain.

Figure 1b. FE Cerebospinal fluid.

The volumetric mesh was then generated from the segmented data and eventually exported to COMSOL Multiphysics for calculation.

The electrical properties of the four compartments were assigned the representative average values taken from standard sources (values in S/m): brain: 0.2; CSF: 1.65; skull: 0.01; skin: 0.465.

The following electrode configurations were simulated:

(1)Distant-bipolar: Stimulation with two disc electrodes placed far apart (> 12 cm; center to center distance) to approximate standard tDCS of the primary motor cortex. This corresponds to placing the active (anode) electrode over motor cortex and the reference (cathode) electrode at the forehead above the contralateral orbita.

(2) 4 X 1 ring configuration: Stimulation with four reference (cathode) electrodes arranged in a circular fashion around an active (anode) center disc electrode. The active electrode is placed over the motor cortex and each of the four reference electrodes are placed (~3 cm) from it (center to center distance).

The disc electrodes had a 4 mm radius and the thickness was 0.5 mm. The electrodes were only energized on the flat distal surface (see below). The electrodes were modeled as conductors with the conductivity of copper (5.8×10^7 S/m). We

do not explicitly consider the use of conductive gels or sponges.

2.2 Mathematical model and Computation

The Laplace equation $\nabla \cdot (\sigma \nabla V) = 0$ (V: potential; σ : conductivity) was solved and the boundary conditions used were (1) inward current flow = J_n (normal current density) applied to the distal surface of the anode electrode, (2) ground applied to the distal surface of the cathode electrode(s) and (3) all other external surfaces treated as insulated. The conductive media DC application mode was used.

The model was adaptively meshed into more than 8,000,000 tetrahedral elements (~ 10,000,000 degrees of freedom) for each of the simulations. The finite element method (FEM) model was implemented using Comsol 3.4 (COMSOL Inc., MA, USA). The linear system solver of conjugate gradients was used with a relative tolerance of 1×10^{-6} .

Figure 2. Volumetric mesh for 4 X 1 ring configuration.

'Surface-magnitude' plots were generated by plotting the magnitude of electric field (E-field) on the top surface of the innermost compartment in the model.

3. Results

For each configuration (Figure 3a and Figure 4a), we obtained the induced E-field in the brain. The 'surface-magnitude' plots of each of the configurations allow a direct comparison of relative spatial focality (Figure 3b and Figure 4b).

The 'Distant-bipolar' stimulation results in relatively diffuse (un-focal) cortical modulation. The current crosses the cortex under each electrode and then traverses the brain stimulating effectively the entire cortical region between the stimulation electrodes (Figure 3c).

Figure 3c. Cross-section slice plot and arrow plot of E-field for Distant-bipolar configuration

The '4 X 1 concentric-ring' configuration leads to significant increases in spatial focality at the expense of increased skin surface current compared to the distant-bipolar configuration.

As expected, reducing the distance between stimulation electrodes increases the current portion shunted through the skull / skin and reduces the current crossing the brain.

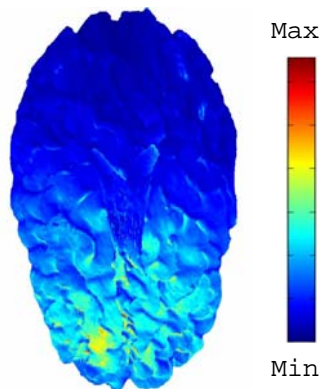**Figure 3a**. Distant Bipolar configuration

Figure 3b. Cortical (brain) surface-magnitude plot of induced E-field for Distant-bipolar configuration.

The plots are normalized to the maximum positive and / or negative to illustrate the extent of stimulation of cortical surface/depth.
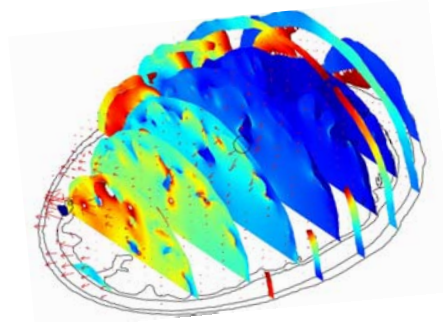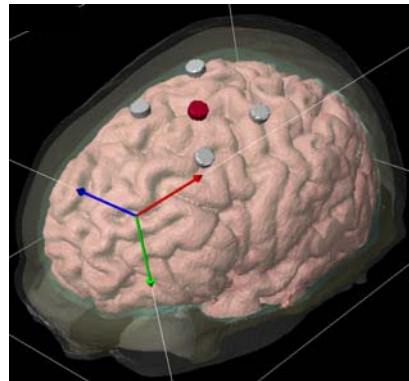

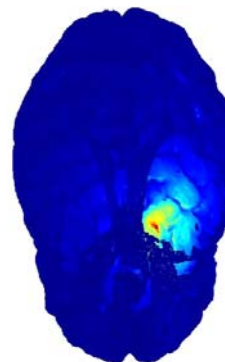**Figure 4a.** 4 X 1Ring configuration

Figure 4b. Cortical (brain) surface-magnitude plot of induced E-field for 4X1 ring configuration.
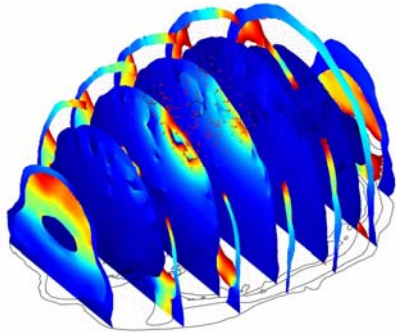
Figure 4c. Cross-section slice plot and arrow plot of E-field for 4 X 1 ring configuration

4. Discussion

Our study compares the spatial extent of induced E-field between the commonly used clinical configuration and the concentric-ring configuration. The results are in accordance with expected results.

Previous modeling studies have not been able to capture neuronal geometry at the cortical gyri/sulci level [8], [9]. Our head model based on highly accurate volumetric meshes allow to observe micro features in the brain (Figure5).
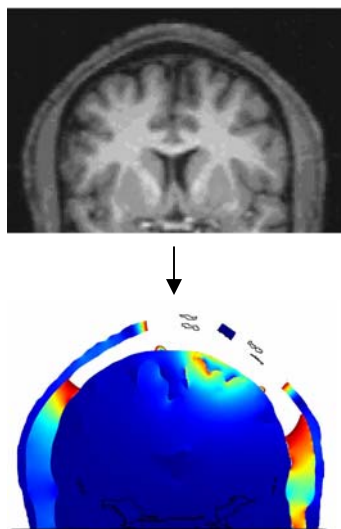

Figure 5. An MRI slice and the corresponding E-field induced in brain/CSF for 4 X 1 ring configuration.

Our model is limited since it incorporates only the four main compartments. Improving the precision of the head model, such as by identifying gray and white matter/skull anisotropy will enhance the accuracy of the electric field profiles.

The results reported here using an optimized electrode configuration (4 X 1 ring) represents an important 'proof-of-principle' supporting further characterization.

Conclusions

This paper presents the induced electric field magnitudes during transcranial current stimulation. The reduced 4 X 1 concentric-ring configuration leads to significant increases in spatial focality compared to commonly used clinical configuration. The concentric-ring may thus provide an optimized configuration for selective targeting of superficial cortical neurons.

8. References

1. M. A. Nitsche and W. Paulus, Sustained excitability elevations induced by transcranial DC motor cortex stimulation in humans, *Neurology*, **57,** 1899-1901 (2001)
2. M. A. Nitsche et al., Level of action of cathodal DC polarization induced inhibition of the human motor cortex, *Clin. Neurophysiol*., **114**, 600-604 (2003)
3. G. Ardolino et al., Non-synaptic mechanisms underlie the after-effects of cathodal transcutaneous direct current stimulaton of the human brain, *J. Physiol.*, **568**, 653-663 (2005)
4. P. Rossini et al., Nervous propagation along 'central' motor pathways in intact man: characteristics of motor responses to 'bifocal' and 'unifocal' spine and scalp non-invasive stimulation, *Electroencephalogr. Clin. Neurophysiol.*, **61**, 272-286(1985)
5. S. S. Nathan et al., Determination of current density distributions generated by electrical stimulation of the human motor cortex, *Electroencephalogr. Clin. Neurophysiol.*, **86**, 183-192 (1993)

6. A. Datta et al., Transcranial current stimulation focality using disc and ring electrode configurations: FEM analysis, *J. Neural Eng.*, **5**, 163-174 (2008)

7. M. Bikson, T. Radman and A. Datta, Rational modulation of neuronal processing with applied electric fields, *Conf. Proc. IEEE Eng. Med. Biol. Soc.*, **1**, 1616-1619 (2006)

8. P.C. Miranda et al., Modeling the current distribution during transcranial direct current stimulation, *Clin. Neurophysiol.*, **117**, 1623-1629 (2006)

9. T. Wagner et al., Transcranial direct current stimulation: a computer based human model study, *Neuroimage*, **35**, 1113-1124(2007)